Stress relaxation in thin films due to grain boundary diffusion and dislocation glide

Ayas, Can

Chapter 6

Development of Intrinsic Stress with Simultaneous Growth and Grain Boundary Diffusion

Intrinsic stress development in thin film/substrate systems during deposition is investigated by discrete dislocation and continuum modelling of grain boundary (GB) diffusion. The transport of material from the free surface into the GBs first relaxes the initially present tensile coalescence stress and subsequently forms a film average compressive stress due to the supersaturation of adatoms on the advancing front of the film. The calculations revealed that if the growth rate is high and/or the columnar grains are wide the magnitude of compressive film average stress is low. The comparison of the continuum predictions are in good agreement with the existing models from the literature when the growth rate is low. However for the high growth rates the agreement is less. The comparisons of DD predictions with the continuum model in [7] gives a qualitative agreement. However the effect of growth rate and grain size is more pronounced in DD calculations. Moreover, the build–in size scale Burgers vector, which is absent in continuum formulations, restricts the minimum admissible width of diffusional displacements along the GB.

[0]Based on *Development of Intrinsic Stress with Simultaneous Growth and Grain Boundary Diffusion*, Can Ayas and E. van der Giessen, in preparation.

6.1 Introduction

One of the important aspects of thin film technology used extensively in small electronic devices is mechanical reliability. Upon manufacturing of a thin film on a substrate, intrinsic stresses arise due to the non-equilibrium nature of the deposition process. The final state of stress depends on the material properties, deposition conditions and the efficacy of relaxation mechanisms present at the length scale of (sub-)micrometers. Beside dislocation plasticity, diffusion of adatoms from the surface into the GBs is a relaxation mechanism that potentially plays a crucial role in the development of intrinsic stress [3].

In Chapter 3, we have analyzed the dislocation–glide mediated relaxation of compressive intrinsic stress that was represented by an array of edge dislocations on the GB. In Chapter 4 the discrete dislocation framework for GB diffusion was developed. The modelling of simultaneous film growth and GB diffusion is the topic of this chapter. The role of the film growth rate and the width of the columnar grains in intrinsic stress development are investigated. Moreover the continuum model presented in Chapter 5 is extended for growing films and its predictions are compared with the existing continuum models in the literature [7, 2].

Volmer-Weber growth of polycrystalline thin films starts with the formation of independent islands on the substrate, which subsequently grow with time. When the distance between islands becomes smaller than a critical value, it is energetically favorable for two neighboring island surfaces to transform into one GB. Upon formation of the GB, islands deform elastically and induce a tensile coalescence stress on the film [8, 5]. As deposition proceeds, a supersaturated adatom population on the top surface creates a compressive stress that pushes adatoms into GBs where the atomic packing is relatively sparse [3]. For most cases the relaxation of tensile coalescence stress is thus followed by the development of a compressive stress. Simultaneously the film grows at a constant growth rate where the free surface moves away from the film–substrate interface.

6.2 Discrete Dislocation Framework

Matter that diffuses into a GB is modelled in terms of discrete dislocations having a Burgers vector perpendicular to the GB. The transport of matter from the surface into the boundaries is represented by the nucleation of dislocations from the free surface, while diffusion along the boundaries is modelled as 'climb-like' motion of the dislocations thus inserted. The reader is referred to Chapter 4 for the governing equations. They are formulated by using Fick's law of diffusion in conjunction with the dissipation of a moving dislocation in terms of the Peach-Koehler force. The driving force for diffu-

sion in this discrete dislocation framework is the component of the Peach-Koehler force normal to the boundary, while the dislocation mobility is determined by the diffusion coefficient.

6.3 Problem Description

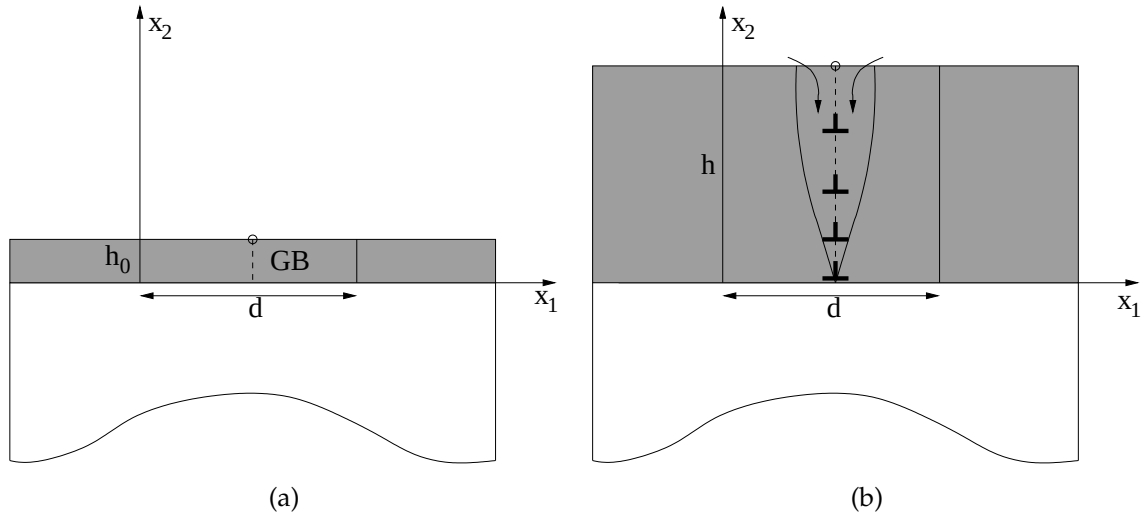

Figure 6.1: Illustration of the coupled growth–diffusion problem. Configuration at the initial stage (a), and at the final stage (b). The source from which the GB dislocations are nucleated are indicated by open circles.

Simultaneous film growth and diffusion is studied in terms of a two-dimensional plane strain problem of an infinitely wide thin film deposited on a very thick elastic substrate, as shown in figure 6.1. The elastic properties (determined by the elastic modulus E and Poisson's ratio ν) of the film and substrate are taken to be identical. Columnar grains of width d are assumed to be growing perpendicular to the film/substrate interface. A computational cell containing a single grain of the film is considered and the infinite film is represented by implementing periodic boundary conditions. The thickness of the film initially is h_0, which increases with time in accordance with a prescribed deposition rate $\dot{h}$.

At the start of growth, a tensile coalescence stress σ_0 is present which evolves due to the competition between growth and relaxation by GB diffusion. Because of the ongoing deposition process, there is a supersaturated adatom concentration at the free surface, which enforces a compressive value for the steady state GB normal stress at the top of the film, σ_s. Since diffusion is driven by the gradients in chemical potential μ, the flux of atoms from the surface to into the GBs,

$$j_{s/gb} \propto (\mu_s - \mu(h)),$$

where $\mu = -\sigma_n \Omega$ (with Ω the volume of an atom, see also Chapter 5). $\mu_s = -\sigma_s \Omega$ denote the chemical potential on the free surface in the presence of the deposition flux. Thus adatoms will continue to flow into GB as long as the $\sigma_n(h) > \sigma_s$.

It bears emphasis that we analyze the stress development during the deposition only. Once the deposition is finished the chemical potential at the free surface will no longer enforce a compressive GB normal stress; instead for a flat surface, $\mu_s = 0$ and hence $\sigma_s = 0$. Therefore the built-in compressive stress would be subjected to relaxation via reverse diffusion of material from the GBs to the free surface. Simultaneously when the film/substrate system is taken out of the deposition chamber to ambient temperature, thermal stresses are likely to develop. Stress relaxation calculations for stationary films were presented in Chapter 4 and Chapter 5. However the current framework is important since the stress developed during the growth may also trigger dislocation glide in slip planes which would complicate the overall mechanism. The reader is referred to Chapter 7 for a first attempt to couple all processes involved: GB diffusion, film growth and dislocation glide.

6.4 Discrete Dislocation Predictions

In this section we study the film stress during the deposition only. For that purpose we have investigated films with various grain sizes subjected to different growth rates. As an example, the development of the film average stress for the central case of a grain size of $d = 0.5$ μm is reported in figure 6.2. The development of intrinsic stress as a function of normalized thickness for other cases will be discussed later in section 6.4 and also in section 6.6. Initially the film is under a homogeneous tensile stress of $\sigma_0 = 250\mathrm{MPa}$ and has thickness $h_0 = 0.02$ μm while $\sigma_s = -250\mathrm{MPa}$. During deposition, the film thickness increases according to $\dot{h}$. The non–dimensional growth rate measure,

$$\dot{H} = \frac{4\pi h_0^2 \dot{h}}{\mathfrak{D} E^*} \tag{6.1}$$

introduced in [7], is used to quantify growth rates relative to the rate of diffusion. The plane strain elastic modulus is denoted by $E^* = E/1 - \nu^2$ and $\mathfrak{D}$ is the effective diffusion coefficient defined in Chapter 4. Along with deposition, diffusion takes place with dislocations nucleation from the free surface and 'climbing' towards the film–substrate interface.

Closed-form expressions for the dislocation stress fields $\tilde{\sigma}_{ij}$ in a periodic half–infinite space [4] are used, so that no extra image forces due to the free surface need to be accounted for. The film average 11–stress, $\langle \sigma_{11} \rangle^f$, is calculated by integrating the total stress, i.e. $\sigma_0 + \tilde{\sigma}_{11}$, over a grid of rectangles with a size of $50\mathrm{nm} \times 80\mathrm{nm}$. Since the film

is growing with time, the uppermost layer of the rectangles are elongated until their thickness becomes twice the original thickness; when this critical thickness is reached the top most rectangles are divided into two in order to carry out integration in an accurate manner.

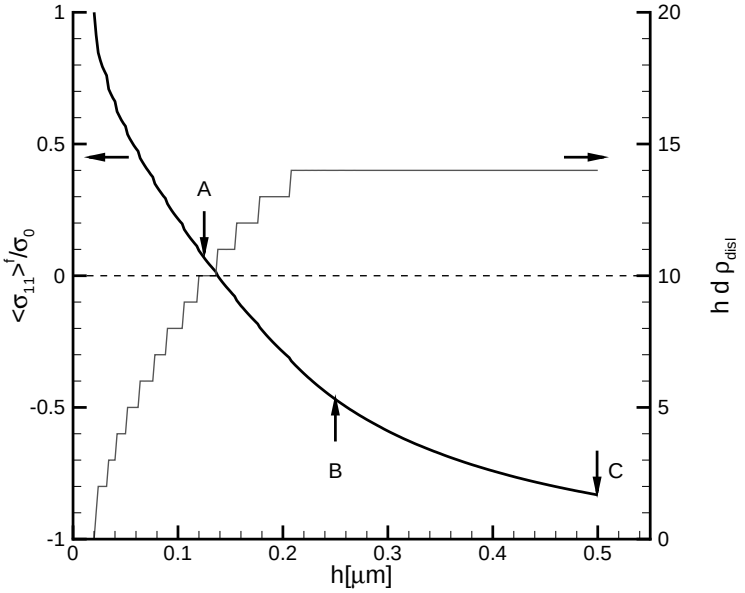

Figure 6.2: Film average stress normalized with initial stress in film/substrate system during deposition (black line). Number of dislocations during the deposition of the film (gray line) $d = 0.50$ and $\dot{H} = 5.4$.

In figure 6.2 the collective 'climb' motion of dislocations in the GB first relaxes the initially present stress. It is followed however, by a build–up of compressive stress dictated by the equilibrium value of normal stress at the GB free surface junction, $\sigma_s = -250\text{MPa}$, and $\dot{H}$. However as we have shown in Chapter 4, even a non–growing film does not attain a uniform stress of σ_s at the steady state. Instead the final state of stress depends on the number and distribution of dislocations present. In order to monitor dislocation nucleation events, the evolution of the total number of dislocations, $hd\rho_{\text{disl}}$ is superimposed in figure 6.2.

The nucleation of a dislocation takes place when the normal stress on the source, which is located h_{nuc} below the free surface, is larger than σ_s and at the same time the 'climb' velocity calculated for a dislocation at the source position is towards the substrate. Our model also takes into account the attraction of dislocations to a nearby free surface through implementation of image stress fields as a function of distance between the dislocation of interest and the free surface (see Chapter 4). The value of h_{nuc} is taken as $24b$ which gives rise to an image stress of approximately -135MPa to a dislocation sitting at the source.

The 11–stress component at the source position, $\sigma_{11}^{(\mathrm{nuc})}$, is plotted against time in figure 6.3. Initially $\sigma_{11}^{(\mathrm{nuc})} = \sigma_0$, but rapid stress drops to compressive values are evidence of dislocation nucleation. After each nucleation event, the stress increases gradually as the dislocation moves away from the source position. As mentioned above, nucleation takes place only when $\sigma_{11}^{(\mathrm{nuc})} > \sigma_s$. However this is a necessary yet not a sufficient condition, since some nucleation events take place only after the 11–stress exceeds σ_s significantly (see figure 6.3).

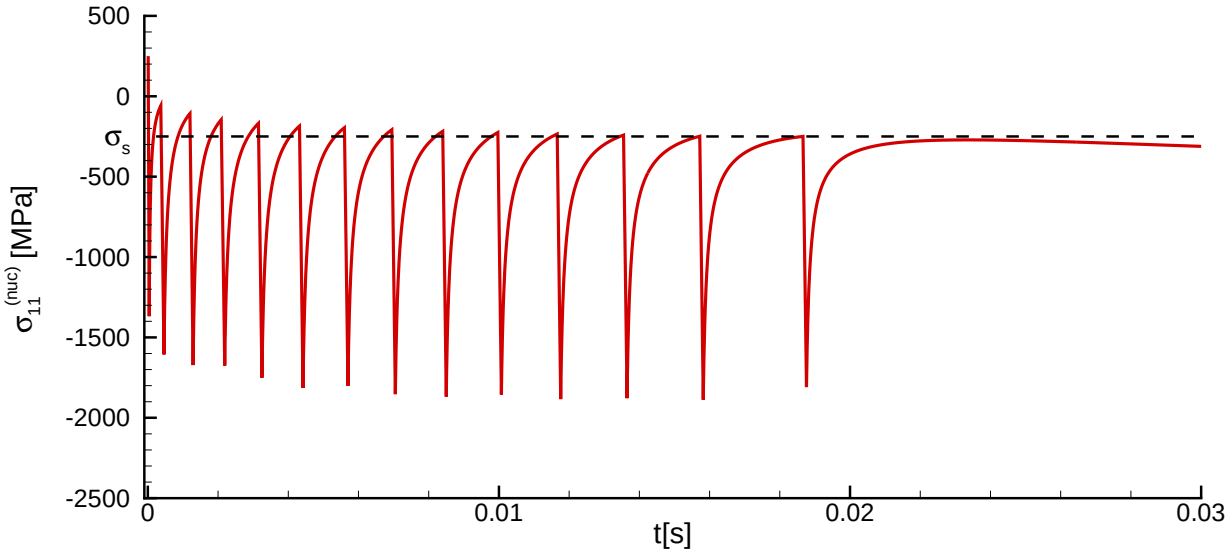

Figure 6.3: 11-stress on the source position for $d = 0.50$ and $\dot{H} = 5.4$.

The distribution of σ_{11} in the film is shown in figure 6.4 at three stages of growth: $h = 0.125$ μm, 0.25 μm and 0.5 μm. The average stress values at these thicknesses are identified in figure 6.2 with the labels A, B and C respectively. For all the films in the close proximity of film/substrate interface, stress levels are closer to σ_0 which marks an unrelaxed region. For the thinnest film, when $h = 0.125$ μm, moving away from interface stress levels decrease and at the top close to the GB a region with compressive stress levels exists. As film growth proceeds together with simultaneous diffusion more dislocations nucleate and they propagate towards the film/substrate interface and the average stress follows the trend given in figure 6.2. When $h = 0.5$ μm the stress distribution is dominated by compressive regions with levels around σ_s with the exception of relatively unrelaxed regions near the substrate.

In figure 6.2 it has been shown that the total number of dislocations becomes constant after a certain thickness and yet the $\langle \sigma_{11} \rangle^f$ continues to decrease and from figure 6.4(b) and 6.4(c) one can observe that the strip of film that is being deposited instantly attains a compressive stress value by feeling the compressive stress field of the

dislocations in the system. This is physically justified by the atomistic picture in which film atoms landing on the film surface replicate the surface crystallography and hence inherit the existing stress. Because of this, dislocation nucleation can be suspended for a certain span of time. However, as growth continues the distance between the free surface and the dislocations will increase and hence $\sigma_n(h)$ will increase which will eventually lead to dislocation nucleation again.

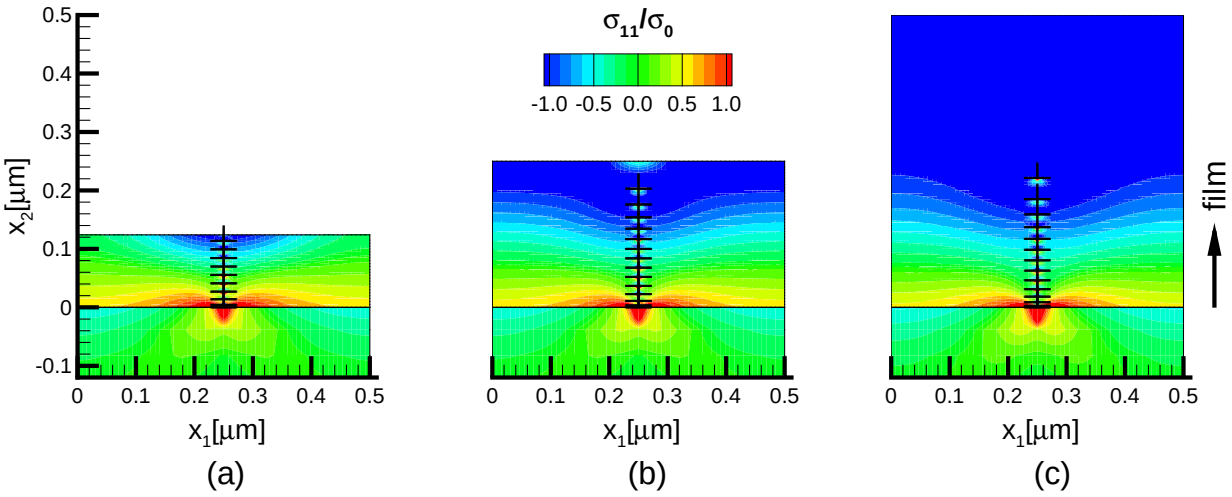

Figure 6.4: Stress distribution during three instances of the growth, $d = 0.50$ and $\dot{H} = 5.4$. The labels A, B and C in figure 6.2 denote the film average stress values corresponding to the stress distributions shown here. Note that $\sigma_0 = -\sigma_s$.

The relaxation and subsequent build up of compressive stress is due to the incorporation of material from the free surface. The extra material creates a GB wedge which is represented by the displacement discontinuity of the GB edge dislocation array. In figure 6.5, by plotting the deformations on the integration grid points, the shape of the GB wedge is illustrated. It reveals that during the initial stages of growth, the free surface of the film is rough (see figure 6.5(a)), which gradually smoothens with further growth (see figure 6.5(b) and (c)). The origin of this surface roughness is the displacement field of dislocations in x_2 direction, $\tilde{u}_2$. When the dislocations are far away from the free surface, as in figure 6.5(c) (see figure 6.4(c) for dislocation configuration at $h = 0.5\mu$m), they do not induce a noticeable roughness.

For a growing film, the grain aspect ratio h/d is a function of time. From the results presented in Chapter 4 and Chapter 5 we know that grains with high aspect ratio are susceptible to more diffusional relaxation; therefore films with small d are expected to have an average compressive stress that is higher in absolute value. Moreover the dimensionless growth rate $\dot{H}$ specifies the competition between the growth and diffusion. The higher the growth rate, the less time is available for diffusional relaxation. Thus:

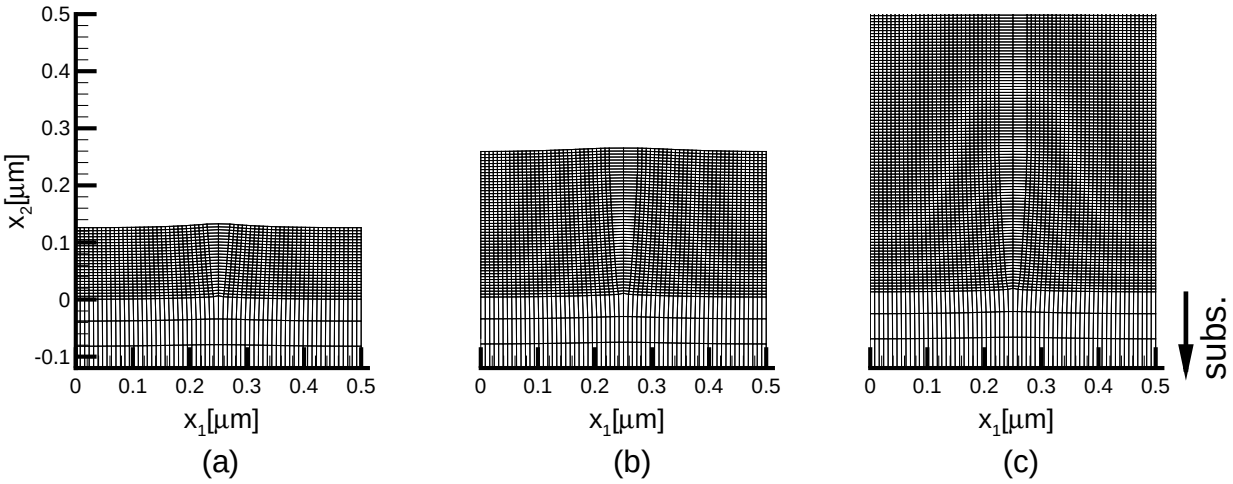

Figure 6.5: Deformed integration grid for thin film with $d = 0.50$ at three instances of growth at $\dot{H} = 5.4$. The labels A,B and C denotes the thickness values that are shown in figure 6.2. Deformations are amplified ten times to improve visibility.

the lower $\dot{H}$, the lower $\langle\sigma_{11}\rangle^f/\sigma_0$ will be.

The scaling of average stress with aspect ratio when the films reach a thickness of $h = 0.5$ μm at different growth rates is given in figure 6.6. When the deposition rate is low the initial tensile stress rapidly relaxes and subsequently a compressive stress builds up as a consequence of diffusion. When growth is fast, diffusion becomes less effective thus giving rise to a weaker compressive stress. For the deposition rates $\dot{H} = 54$ and $\dot{H} = 5.4$, some average tensile stress persists for $d = 2$ μm when the film has reached a thickness of $h = 0.5$ μm ($h/d = 0.25$).

6.5 Continuum Models

A number of continuum models have been proposed in the literature for intrinsic stress development via GB diffusion. The different features of the existing continuum models related with this problem are summarized in table 6.1. The simplest one is the 'linear spring' (LS) model presented in [7]. In this model the diffusion of material to the GB is represented by the opening between neighboring grains, $\Delta(x_2)$, which is accommodated by elastic strain in the grains. The compatibility condition then leads to

$$\sigma_n(x_2) = -\frac{\Delta(x_2)}{E^* d}, \tag{6.2}$$

which is used to conceptually replace elastic grains with linear springs. The stress in the film develops according to Fick's law. The boundary conditions considered are flux

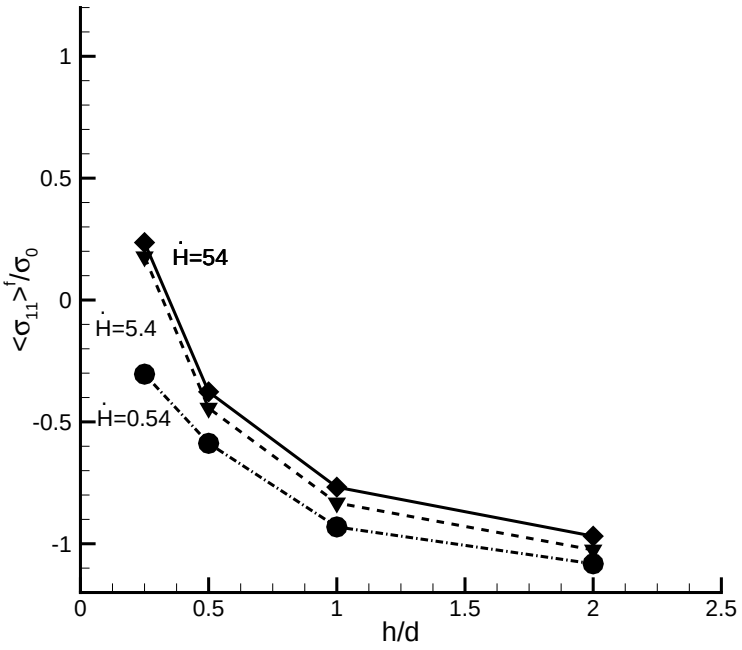

Figure 6.6: Overall normalized intrinsic stress at the end of deposition ($h = 0.5\ \mu$m) against grain aspect ratio h/d for different grain size and deposition rates.

continuity at the free surface and zero flux at the film/substrate interface. Although the film is bonded to a substrate the boundary condition that enforces the GB opening to be zero at the film/substrate interface has been omitted in [7] for the sake of the simplicity. Since the model is one dimensional, the film average stress is not well defined; in [7] it is found from the stress averaged over the GB, $\langle\sigma_{11}\rangle^{gb}$, with the term $f(h/d)$ as

$$\langle\sigma_{11}\rangle^{f} = \sigma_0 + \underbrace{\frac{4h}{d}\tanh\left(\frac{4h}{d}\right)}_{f(h/d)}\Big(\langle\sigma_{11}\rangle^{gb} - \sigma_0\Big). \tag{6.3}$$

The function $f(h/d)$ is based on the energy release rate at each crack tip for steady state channeling of infinite array of parallel mode I film cracks in the direction normal to the plane of deformation [9]. Unfortunately the connection between the energy release rate and stress decay away from the GB in x_2 direction has not been explained in detail.

The second framework is the continuum dislocation (CD) model developed for stationary films in [6] and extended for film growth in [7, 2]. The evolution of dislocation distribution is governed by the diffusion law and describe the volumetric flux along the GB in the same spirit as in the DD model. Although the physical boundary conditions are fully taken into account, this model is also one dimensional and hence the stress averaging over the film is carried out in the same way as in the LS model by multiplying $\langle\sigma_{11}\rangle^{gb}$ with $f(h/d)$ as in equation (6.3) [7, 2].

	BCs	grain model	stress averaging	GB Wedge
LS [7]	$j_2(0) = 0$	$\sigma_{11} = \dfrac{-E^* \Delta(x_2)}{d}$	$\langle \sigma_{11} \rangle^f = \sigma_0 + \dfrac{f(h/d)}{h} \displaystyle\int_0^h (\sigma_n - \sigma_0)\, dx_2$	$0 < \Delta(x_2)$
CD [7, 2]	$j_2(0) = 0$ $\Delta(0) = 0$	$\sigma_{ij} = \mathfrak{L}_{ijkl} \varepsilon_{kl}$	$\langle \sigma_{11} \rangle^f = \sigma_0 + \dfrac{f(h/d)}{h} \displaystyle\int_0^h (\sigma_n - \sigma_0)\, dx_2$	$0 < \Delta(x_2)$
SC [1]	$j_2(0) = 0$ $\Delta(0) = 0$	$\sigma_{ij} = \mathfrak{L}_{ijkl} \varepsilon_{kl}$	$\langle \sigma_{11} \rangle^f = \dfrac{1}{dh} \displaystyle\int_0^d \int_0^h \sigma_{11}\, dx_2 dx_1$	$0 < \Delta(x_2)$
DD	$j_2(0) = 0$ $\Delta(0) = 0$	$\sigma_{ij} = \mathfrak{L}_{ijkl} \varepsilon_{kl}$	$\langle \sigma_{11} \rangle^f = \dfrac{1}{dh} \displaystyle\int_0^d \int_0^h \sigma_{11}\, dx_2 dx_1$	$b < \Delta(x_2)$

Table 6.1: Basic features of models for intrinsic stress development in the literature. First column gives the boundary conditions (BCs) at the film/substrate interface, second column describes the constitutive model for the grains, third column tabulates the way stress averaging is carried out and the forth column gives the lower limit for $\Delta(x_2)$ values.

In Chapter 5 we have proposed a staggered continuum (SC) model which takes into account all the physically important boundary conditions and constructed in a fully two dimensional way. The coupling between elasticity and diffusion is dealt within a staggered numerical solution of diffusional and linear elastic boundary value problems. For GB diffusion a finite difference scheme is used while the elasticity problem is solved by the finite element method. Stress averaging is carried out by numerically integrating the stress over the film. This model can also be extended for growing films where simultaneous diffusion and film growth can be studied. For this purpose the film thickness is increased at every time step in accordance with $\dot{h}$ and the GB is re–meshed with the same number of finite difference nodes having a uniform separation. The values of $\Delta(x_2)$ at new nodal positions are found by linear interpolation from the former positions. For the linear elastic BVP the film domain is also re-meshed at every time step so that the finite element nodes overlap with the moving finite difference grid on the GB. A disadvantage of this scheme is its computational expense associated with assembling the finite element stiffness matrix at every time step during the calculation. Therefore the growth of the film can be simulated for small changes in film thickness whereas for instance the LS model is computationally very efficient since it is solely based on a Eulerian finite difference diffusion discretization [7]. Adaptation of the numerical scheme to improve the computational efficiency are certainly possible but are not pursued here.

The predictions of the staggered continuum (SC) model with the parameters reported in [7] are plotted with solid curves in figure 6.7. In order to facilitate the comparisons, the predictions of the LS model are reproduced from [7] and drawn with dashed lines. In accordance with that reference, figure 6.7(a) depicts a normalized stress multiplied by thickness (i.e., film force per unit depth) against the normalized thickness, h/h_0. The normalized stress measure is based on the GB normal stress measure s_{ave},

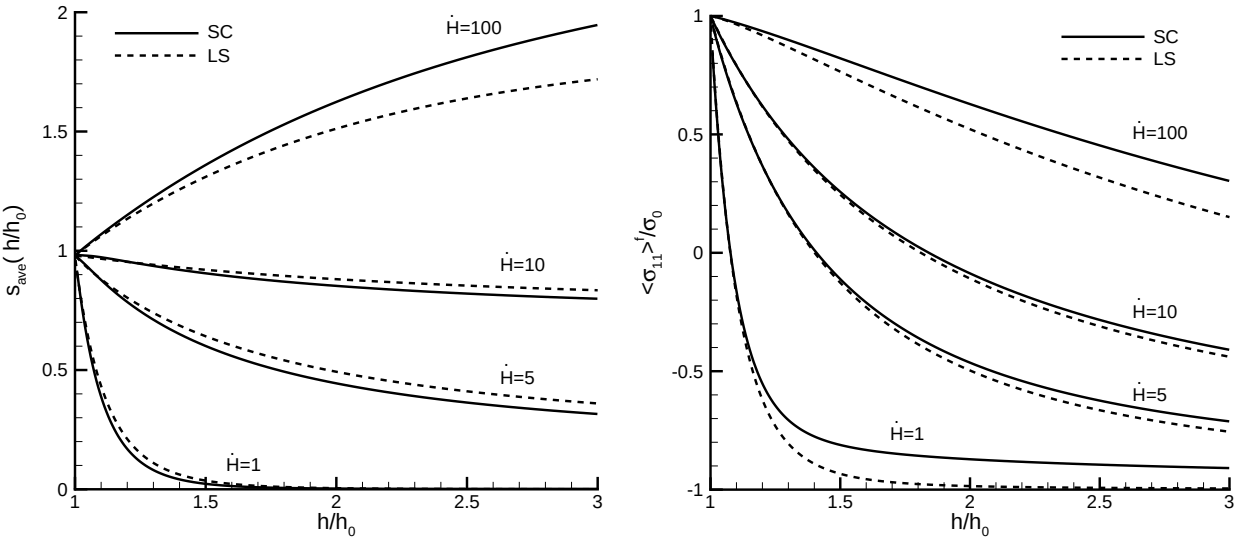

Figure 6.7: Comparison of the predictions by the Staggered Continuum (SC) and the Linear Spring (LS) model. Normalized stress $\times$ thickness evolution as a function of normalized film thickness h/h_0 (a). The development of film average stress normalized with the initial stress (b).The initial film thickness and grain size are taken to be $h_0 = d = 0.125$ μm.

defined by

$$s_{\text{ave}} = \int_0^h \frac{\sigma_n(x_2) - \sigma_s}{\sigma_0 - \sigma_s} dx_2. \tag{6.4}$$

Except for the highest growth rate, the normalized film force decreases with h, since GB diffusion has been effective in stress relaxation. For the highest growth rate $\dot{H} = 100$, diffusion has been much more limited for either of the two models. As a consequence, the product $s_{\text{ave}} \times h/h_0$ shows an increasing trend during growth since the reduction in average normalized stress s_{ave} is overruled by the increase of film thickness.

The comparison in figure 6.7(a) reveals that the SC model leads to films having slightly more extra material and therefore lower compressive stress for slow and moderate growths. There is a larger disagreement between the models for high growth rates. For the highest growth rate $\dot{H} = 100$, the ordering of the solid and dashed curves actually has changed, denoting less stress relaxation for SC model compared to LS model. We have checked that this is not due to spatial or temporal resolution of the numerical techniques involved. The prediction of our SC model seems to be also in perfect agreement with the CD model at the lowest growth rate considered, cf. figure 6 in [7]. Again at high growth rates the agreement become less good. The origin of this difference at high $\dot{H}$ values is unknown.

In figure 6.7(b) stress averaging for the SC model is carried out by proper numer-

ical integration whereas for the LS model $\langle\sigma_{11}\rangle^{gb}$ is converted to film average stress through equation (6.3). It is important to note that the previous comparison based on figure 6.7(a) does not take into account the different stress averaging schemes of the SC and the LS models. We observe that the two averaging schemes give quite significant differences such that, for instance, nearly overlapping solid and dashed lines in figure 6.7(a) for $\dot{H} = 1$ are separated apart in figure 6.7(b). Comparing the solid and dashed curves in figure 6.7(b) we see that the LS model overestimates stress relaxation at all growth rates considered.

6.6 Discrete Dislocation vs. Linear Spring Model

The common feature of all the continuum models is the absence of an innate length scale which designates the minimum admissible $\Delta(x_2)$. Therefore the GB wedge width can be infinitely small. In contrast, the DD model has a built-in length scale b which constrains $\Delta(x_2)$ to be only integer multiples of b (see table 6.1).

In figure 6.8(a) the film average stress development is calculated with the DD model while in figure 6.8(b) the predictions of the LS model are given. There is a qualitative agreement between the models in the sense that higher $\dot{H}$ values give rise to lower compressive stress, and that for a given $\dot{H}$ the magnitude of the compressive stress increases when the grain size d decreases (higher h/d). Given the fact that the assumptions and the construction of the two models are different in various aspects (see table 6.1), it is difficult to point out where the quantitative discrepancies arise from. At any rate, one notable difference is that the effects of $\dot{H}$ and d are more pronounced in the DD model leading to more distinct differences in the final stress values.

Another difference that deserves attention is the stress development in narrow grains ($d = 0.25$ μm). Except at the highest growth rate considered ($\dot{H} = 54$), the DD model predicts that $\langle\sigma_{11}\rangle^{f}$ can become slightly smaller than σ_s in the late stages of growth (see figure 6.8(a)). In the LS model, the final stress is never smaller than σ_s even when the growth rate is lower than the one shown in figure 6.8. This difference is connected to the built-in size scale of the DD model. Since in a continuum framework, the GB can accommodate any displacement, the mass flux at the advancing front of the film is adjusted to inject the necessary amount of material according to the corresponding normal stress gradient. However, in DD, the material flux from the surface into the GB is quantized by dislocation nucleation. Therefore when all dislocations in the film are in equilibrium positions and yet the nucleation criterion is still satisfied, an extra dislocation will be put into the system and the average stress value can exceed σ_s in magnitude. In the LS framework, diffusion in such a state can be far less.

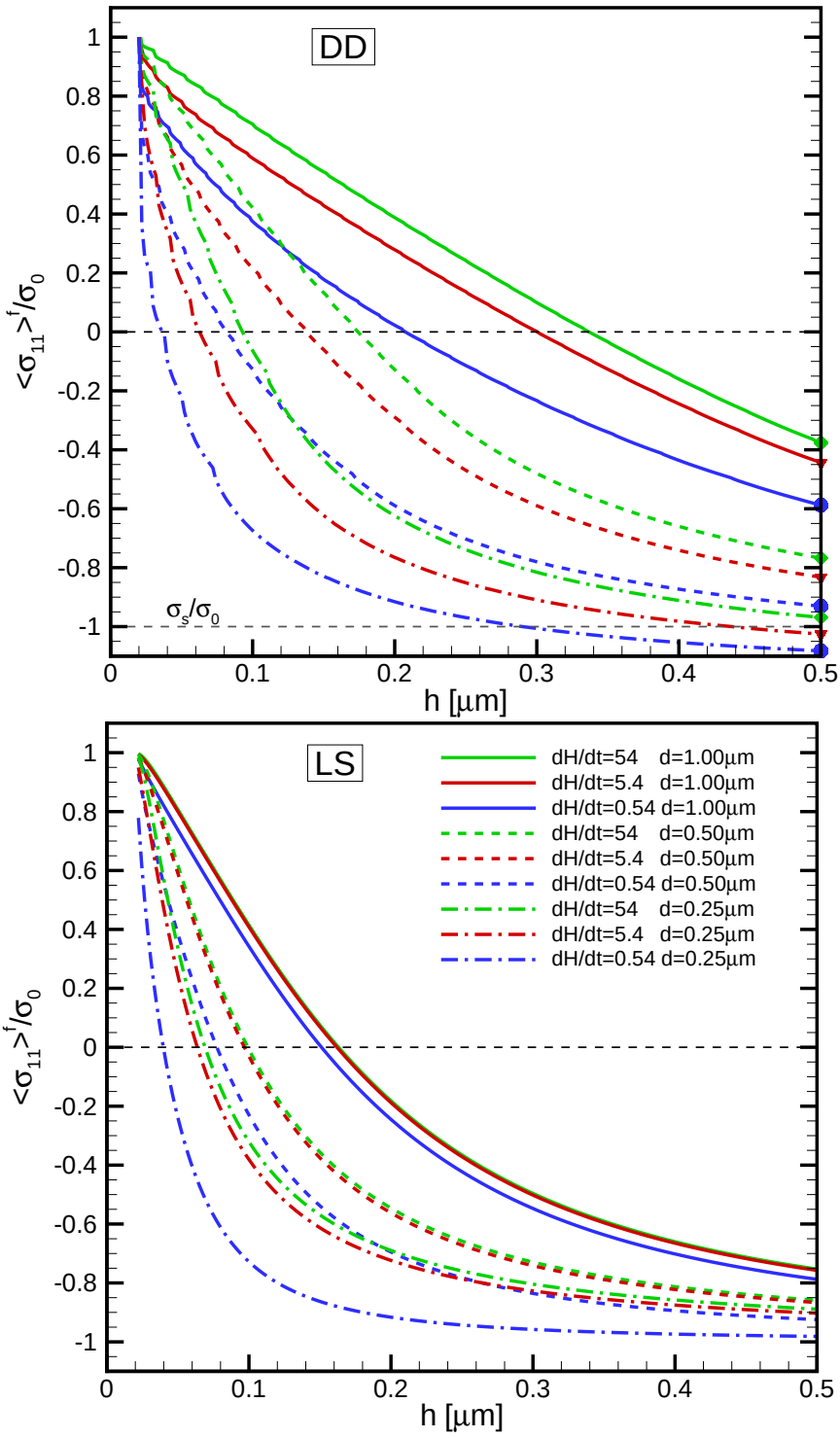

Figure 6.8: DD predictions (a) compared with (b) the linear spring (LS) model from Guduru *et al.* [7]. The film average stress values at $h = 0.5\,\mu$m are labeled with different symbols according to $\dot{H}$ in (a) which were previously shown in figure 6.6. The value of the kinetic parameter A defined in [7] is taken as $A = 3.3$.

Bibliography

[1] C. Ayas and E. Van der Giessen. A continuum framework for grain boundary diffusion in thinfilm/substrate systems. *Journal of Applied Physics*, Accepted, 2010.

[2] T.K. Bhandakkar, E. Chason, and H. Gao. Formation of crack like diffusion wedges and compressive stress evolution during thin film growth with inhomogeneous grain boundary diffusivity. *International Journal of Applied Mechanics*, 1:1–19, 2009.

[3] E. Chason, B.W. Sheldon, L.B. Freund, J.A. Floro, and S.J. Hearne. Origin of compressive residual stress in polycrystalline thin films. *Physical Review Letters*, 88(15), Apr 2002.

[4] L.B. Freund. The mechanics of dislocations in strained-layer semiconductor materials. In John W. Hutchinson and Theodore Y. Wu, editors, *Advances in Applied Mechanics*, volume 30, pages 1 – 66. Elsevier, 1993.

[5] L.B. Freund and E. Chason. Model for stress generated upon contact of neighboring islands on the surface of a substrate. *Journal Of Applied Physics*, 89(9):4866–4873, May 2001.

[6] H. Gao, L. Zhang, W.D. Nix, C.V. Thompson, and E. Arzt. Crack-like grain-boundary diffusion wedges in thin metal films. *Acta Materialia*, 47(10):2865 – 2878, 1999.

[7] P.R. Guduru, E. Chason, and L.B. Freund. Mechanics of compressive stress evolution during thin film growth. *Journal of the Mechanics and Physics of Solids*, 51:2127–2148, 2003.

[8] R.W. Hoffman. Stresses in thin films: The relevance of grain boundaries and impurities. *Thin Solid Films*, 34:185 – 190, 1976.

[9] Z.C. Xia and J.W. Hutchinson. Crack patterns in thin films. *Journal of the Mechanics and Physics of Solids*, 48(6-7):1107 – 1131, 2000.